Journal of the Korean Society of Propulsion Engineers
Vol. 20, No. 5, pp. 40-50, 2016

Research Paper DOI: http://dx.doi.org/10.6108/KSPE.2016.20.5.040

나노 알루미늄/불소 함유 폴리우레탄 결합제의 합성 및 열적 특성 연구

Qianqian Lan[a] · 김진석[b] · 권영환[a,*]

Synthesis and Thermal Characteristics of Nano-Aluminum/Fluorinated Polyurethane Binders

Qianqian Lan[a] · Jin Seuk Kim[b] · Younghwan Kwon[a,*]
[a]*Department of Chemical Engineering, Daegu University, Korea*
[b]*Agency for Defense Development, Korea*
[*]*Corresponding author. E-mail: y_kwon@daegu.ac.kr*

ABSTRACT

Energetic plasticizers containing explosophore groups such as $-NO_2$, $-ONO_2$, and $-N_3$ group are susceptible to impact, shock, heat, etc, finally deteriorating the insensitivity of PBXs. In this study, in an attempt to investigate the feasibility of replacing sensitive explosophore groups to fundamentally inactive but potentially (latent) energetic fluorine group which was known to have an exothermic thermite reaction with aluminum, nano-aluminum/fluorinated polyurethane binders were prepared by simultaneous polyurethane and catalyst-free azide-alkyne click reaction in the presence of nano-aluminum. Thermal characteristics of nano-aluminum/fluorinated polyurethane binders were monitored by using DSC with high pressure crucible pan.

초 록

현재 적용되고 있는 에너지화 가소제는 $-NO_2$, $-ONO_2$ 및 $-N_3$와 같은 에너지화 활성 그룹을 포함하고 있어서 충격, 쇼크, 열 등 외부환경에 상당히 민감하여 복합화약의 둔감 안정성을 취약하게 한다. 본 연구에서는 민감한 에너지화 활성 그룹이 아니라 근본적으로는 비활성 그룹으로 복합화약의 민감도에는 영향을 미치지 않지만, 복합화약의 반응 시에 테르밋반응에 의해 추가적인 에너지를 발생할 수 있는 불소계 반응성 가소제를 적용한 폴리우레탄 결합제를 클릭반응으로 합성하고 나노 알루미늄과의 테르밋반응에 대한 열적 특성을 고찰하였다.

Key Words: Nano Aluminum(나노알루미늄), Fluorinated Binder(불소계결합제), Thermite Reaction (테르밋반응), Click Reaction(클릭반응)

Received 1 August 2016 / Revised 6 September 2016 / Accepted 12 September 2016

pISSN 1226-6027 / eISSN 2288-4548

1. Introduction

Energetic plasticizers have gained a lot of

interest as one of important components in solid propellant and plastic bonded explosives, because they improve the processability of energetic material formulations, modulate the thermal and mechanical properties for improving safety characteristics, and contribute to the enhancement of the final energetic performances [1,2]. One of disadvantages of energetic plasticizers stems from explosophore groups such as nitrate ester ($-ONO_2$), azide ($-N_3$), and nitro ($-NO_2$) groups [3,4], which are necessarily incorporated into the structure of energetic plasticizers in order to increase the energetic performance. However, the explosophore groups generally show high impact sensitivity, instability at high temperature or easy oxidation under air atmosphere, and these properties cause the safety issues during the process of manufacture, transportation, usage and storage of energetic materials. In order to eliminate the safety issues caused by explosophore groups, therefore, it is still of importance to study exceptionally stable energetic source for energetic plasticizers.

The use of fluorine or its derivatives as oxidizers in various propellants, explosives and pyrotechnics has been recognized [5]. Therefore, metal/fluorocarbon-based energetic materials have been developed with a great number of applications. In metal/fluorocarbon systems, the enthalpy of formation of the metal-F bond is the driving force behind oxidation of the metal, resulting in the exothermic release of energy called as "thermite reaction". For instance, the reaction of aluminum (Al) with teflon generates 21 GJ/m^3 [6]. As reported in Table 1 [7], the energy density of certain Al-based thermite mixtures have higher mass and volumetric energy density than high explosives. Several

Table 1. Mass and volumetric energy density of thermite mixtures along with some common explosives.

Materials	ΔH_{volume} (kJ/cc)	ΔH_{mass} (kJ/g)
Metal oxidizer		
Al/MoO_3	17.78	4.60
Al/Ni_2O_3	8.37	4.60
Al/Teflon	19.87	8.78
$Al/KClO_4$	27.20	10.46
High explosive		
TNT	7.53	5.02
HMX	10.88	5.23
PETN	10.46	6.28
CL-20	16.74	7.95

Al/fluorocarbon systems have been developed including Al/PTFE [8], Al/PVDF [9], and Al/perfluoropolyether in epoxy [10].

This article presents new type of polyurethane (PU) binders containing fluorine groups as a potential energetic group to increase the energetic performance by utilizing the thermite reaction with Al, because Al has been currently used in many formulations of propellants and plastic bonded explosives. Thermal characteristics of nano-aluminum/ fluorinated polyurethane binders were monitored by using DSC with high pressure crucible pan.

2. Experimental

2.1 Materials

4,4,5,5,6,6,6-Heptafluorohexanoic acid (HFHA, 97%) was purchased from Matrix Scientific. Propagyl alcohol (PPA, 99%), p-toluenesulfonic acid monohydrate (p-TsA, 98.5%), 3,5-dinitro salicylic acid (DNS, 98%), 1,3,5-trioxane (≥ 99%) and 2,2,3,3,4,4,5,5-octafluoro-1-pentanol (OFP-OH, 98%) were purchased from

Sigma-Aldrich Co. 3-Butyn-1-ol (BTO, 98%) was purchased from Alfa Aesar Co. Aluminum nanopowder (n-Al, 99.9+%) was purchased from US Research Nanomaterials, Inc. Deuterated chloroform ($CDCl_3$, 99.8%) was supplied by Merck KGaA. Triphenyl bismuth (TPB), isophorone diisocyanate (IPDI) and Desmodur® N-100 were supplied by ADD. Poly(glycidyl azide-co-tetramethylene glycol) (glycidyl azide to tetramethylene glycol mole ratio: 3/7 and 5/5) (PGT(3/7) and PGT(5/5)) were supplied by Hepce Chem. Co.

2.2 Instruments

^1H and ^{13}C-NMR spectra were recorded on a NMR spectrometer (300 MHz, Varian Mercury). Chemical shifts were reported as δ parts per million with reference to tetramethylsilane (TMS) as internal standard.

The tensile strength, ultimate elongation and modulus were measured on a universal test machine (TO-100-IC, Test One) with a 50 kg_f load cell and software (Test One_UTM Version 12.0.2). The rate of tensile was 0.8 mm/s. The tensile test samples were cut from the cast film with spec (DIN-53504, type (S2)). All reported results for the tensile strength, ultimate elongation and initial modulus were averages of 3 measured values.

Thermogravimetric analysis was performed with TGA (TGA4000, PerkinElmer) with a heating scan rate of 20°C/min in the temperature range of 50°C to 900°C with the N_2 flow rate of 20 ml/min. The sample weight was about 5 mg to 10 mg. The maximal decomposition temperature ($T_{d,max}$) was defined as a temperature when the maximum rate of weight loss occurred, and obtained from DTG curve.

Glass transition temperature (T_g) was measured with differential scanning calorimetry (DSC8000, PerkinElmer) in a nitrogen atmosphere (20 ml/min) at a heating rate of 10°C/min in the temperature range of -120°C to 0°C. All reported T_gs were the temperature in the middle of the transition.

Energetic performance was investigated by using DSC (DSC821e, Mettler). All tests were performed in a nitrogen atmosphere (20 ml/min) at a heating rate of 10 °C/min in the temperature range 50 ~ 600°C. Al crucible and high pressure crucible (M50, TUV-SUV) were used.

Heat of combustion was determined using a Parr Bomb calorimeter (Parr 6100 calorimeter, Parr instrument company). Samples weighing 0.5g were placed in a metal crucible in the parr 1108 oxygen combustion bomb. The bomb was sealed, filled with pure oxygen, connected to the parr ignition unit, and placed in a parr oxygen bomb calorimeter in a water bath. A thermocouple inserted in the water bath measured temperature during the experiments.

2.3 Synthesis of fluorinated reactive plasticizers (FRPs)

Ester-linkage FRPs: Reaction scheme is shown in Fig. 1. A mixture of HFHA (10 mmol), PPA or BTO (15 mmol) and p-TsA (1 mmol) was dissolved in toluene (20 mL) and heated in a one-necked round bottom flask equipped with condenser kept 110 °C for 12 h. After reaction, the cooled solution was diluted by EA and then washed by saturated aqueous $NaHCO_3$ solution (20 mL) three times. The organic extracts were dried by $MgSO_4$ and the solvent was removed by rotary evaporators. The final crude product was purified by column chromatography (silica gel, EA/hexane (v/v) = 1/10).

Prop-2-yn-1-yl 4,4,5,5,6,6,6-heptafluorohexanoate (E-7F-1, n=1). ^1H NMR (300 MHz, $CDCl_3$, ppm): δ = 2.33-2.59 (m, 1H, 2H, -C≡C-H,

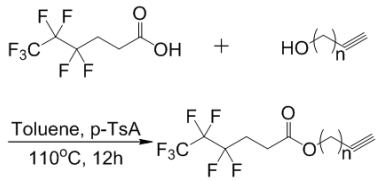

Fig. 1 Reaction scheme for synthesis of ester-linkage FRPs; E-7F-1 (n=1) and E-7F-2 (n=2).

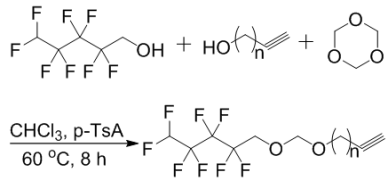

Fig. 2 Reaction scheme for synthesis of formal-linkage FRPs; F-8F-1 (n=1) and F-8F-2 (n=2).

-C-CH_2-C-), 2.59-2.73 (t, 2H, -C-CH_2-C-), 4.65-4.72 (m, 2H, -CH_2-C≡C-). ^{13}C NMR (75 MHz, $CDCl_3$, ppm) δ=170.24, 105.37-121.62, 77.06, 75.07, 52.43, 26.23, 25.09.

But-3-yn-1-yl 4,4,5,5,6,6,6-heptafluorohexanoate (E-7F-2). ^{1}H NMR (300 MHz, $CDCl_3$, ppm): δ = 1.92-1.98 (t, 1H, -C≡C-H), 2.28-2.54 (m, 2H, 2H, -C-CH_2-C-, -CH_2-C≡C-), 2.54-2.67 (t, 1H, -C-CH_2-C-), 4.11-4.20 (m, 2H, -O-CH_2-C-). ^{13}C NMR (75 MHz, $CDCl_3$, ppm) δ=170.67, 108.24-120.85, 79.65, 69.83, 62.48, 26.15, 25.29, 18.64.

Formal-linkage FRPs: Reaction scheme is shown in Fig. 2. A mixture of OFP-OH (8.62 mmol), p-TsA (0.86 mmol) and 5 ml chloroform was stirred in a two-necked round bottom flask at 60°C. 10 ml chloroform, PPA or BTO (8.62 mmol) and trioxane (2.87 mmol) were dropwise added by an automatic injector during 6 hours. After reaction, the solvent was removed by rotary evaporators and then diluted by EA. The solution was washed by 5% $NaHCO_3$ aqueous solution followed with deionized water for three times. The organic extracts were dried by $MgSO_4$ and the solvent was removed by rotary evaporators. The final crude product was purified by column chromatography (silica gel, EA/hexane (v/v) = 1/10).

1,1,2,2,3,3,4,4-Octafluoro-5-((prop-2-yn-1-yloxy)methoxy)pentane (F-8F-1, n=1). ^{1}H NMR (300 MHz, $CDCl_3$, ppm): δ=2.39-2.48 (t, 1H, -C≡C-H), 2.91-4.13 (t, 2H, -C-CH_2-O-), 4.17-4.29 (m, 2H, -CH_2-C≡C-), 2.17-4.29 (s, 2H, -O-CH_2-O-), 5.82-6.26 (m, 1H, -CHF_2-C-). ^{13}C NMR (75 MHz, $CDCl_3$, ppm) δ=104.41-118.80, 94.27, 78.42, 74.94, 64.24, 54.86.

5-((But-3-yn-1-yloxy)methoxy)-1,1,2,2,3,3,4,4-octafluoropentane (F-8F-2, n=2). ^{1}H NMR (300 MHz, $CDCl_3$, ppm): δ=1.92-1.99 (t, 1H, -C≡C-H), 2.36-2.47 (m, 2H, -C-CH_2-C≡), 3.54-3.71 (m, 2H, -O-CH_2-C-), 3.94-4.09 (t, 2H, -C-CH_2-O-), 4.65-4.77 ppm (s, 2H, -O-CH_2-O-), 5.78-6.22 (m, 1H, -CHF_2-C-). ^{13}C NMR (75 MHz, $CDCl_3$, ppm) δ=103.80-118.81, 95.72, 80.88, 68.94, 66.54, 63.95, 19.83.

2.4 Synthesis of n-Al/FRP-incorporated PGT-based PU binders

Reaction scheme is presented in Fig. 3. PGT prepolymer (3.50 g, 2.65 mmol) was dried by a vacuum oven at 60°C overnight. The dried PGT was added into the reactor, kept stirring at the temperature of 60°C in vacuum for 1 h, then cooled down to 30°C for 0.5 h. The vacuum was released and IPDI (0.21 g, 1.86 mmol) and N-100 (0.18 g, 0.93 mmol) was rapidly added into reactor. After stirring for 0.5 h at 30°C, 0.27 g of TPB solution (20 wt% in benzene), 0.47 g of DNS solution (12.5 wt% in benzene) and E-7F-1 (3.68 g, 13.11 mmol) were added and stirred for another 0.5 h under vacuum. The vacuum was released and n-Al (1.44 g, 53.19 mmol) was added into reactor and stirred for 0.5 h under vacuum. After that, the mixture was cast into a mold (3 cm × 8 cm) and kept in an oven at 30°C

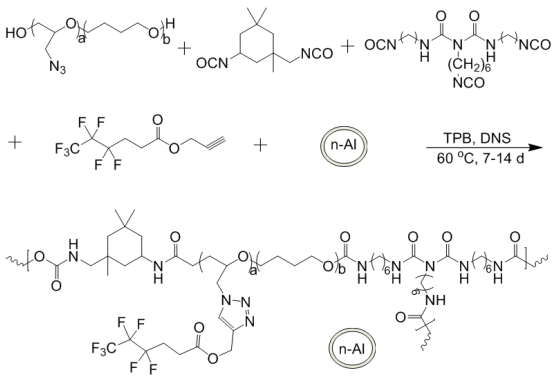

Fig. 3 Reaction scheme for synthesis of E-7F-1-incorporated PGT-based PU binder with n-Al.

to remove the bubble under vacuum for 3 h. Then the mold was moved to an oven at 60 °C for 7-14 days.

3. Results and Discussion

3.1 Thermal properties

Ester-linkage and formal-linkage FRPs were respectively synthesized and characterized as shown in Fig. 1 and Fig. 2. Two ester-linkage FRPs, E-7F-1 and E-7F-2, were synthesized using normal esterification. Formal-linkage FRPs, F-8F-1 and F-8F-2, were prepared by an acetalization reaction. In these FRPs, the "E" and "F" are ester- and formal-linkage, "7F" and "8F" present the number of fluorine atoms, and "1" and "2" are a number of methylene spacer between the formal- or ester-linkage and the alkyne group in FRPs. The propargyl (n=1) and 3-butynyl (n=2) moieties in FRPs were selected as the active site for the click reaction, because these moieties activated by neighboring electron withdrawing ester and formal groups can allow Cu(I)-free 1,3-dipolar cycloaddition with azide groups being completed, even without an interruption of polyurethane reaction [11].

Because the use of high temperature (> 100°C) and Cu catalyst for click reaction might have an adverse effect on PU reaction as well as long-term stability of the energetic compositions, we used in-situ combination of PU reaction and azide-alkyne click reaction at 60°C in the absence of Cu catalyst [11]. As presented in Fig. 3, n-Al/FRP-incorporated PGT-based PU binders were successfully prepared using polyurethane reaction of hydroxyl-terminated PGT prepolymer with IPDI and N-100 curing agents, and simultaneous Cu-free azide-alkyne click reaction of azide groups in PGT prepolymer with alkyne groups in FRPs in the presence of n-Al.

Glass transition temperature (T_g) has been an important parameter as thermal property of materials. Given to the application, the PU binders are preferred to have low T_g. T_gs of PGT prepolymers, PGT-based PU, FRP-incorporated PU, and n-Al/FRP-incorporated PGT-based PU were all measured and summarized in Table 2. Among them, Fig. 4 presents a representative DSC curves of series of n-Al/(E-7F-1)-incorporated PGT(3/7)-based PU binders. T_gs of PGT(3/7) prepolymer, PGT(3/7)-based PU, (E-7F-1)-incorporated PGT(3/7)-based PU and n-Al/(E-7F-1)-incorporated PGT(3/7)-based PU were -87.6°C, -63.7°C, -39.8°C and -27.5°C. T_g of (E-7F-1)-incorporated PGT(3/7)-based PU was higher than that of PGT(3/7)-based PU, which was associated with the formation of triazole side group via azide-alkyne click reaction. The addition of n-Al further increased T_g of (E-7F-1)-incorporated PGT(3/7)-based PU.

As appeared in Fig. 5, series of n-Al/(E-7F-1)-incorporated PGT(5/5)-based PU binders are similar trend in T_g variation of

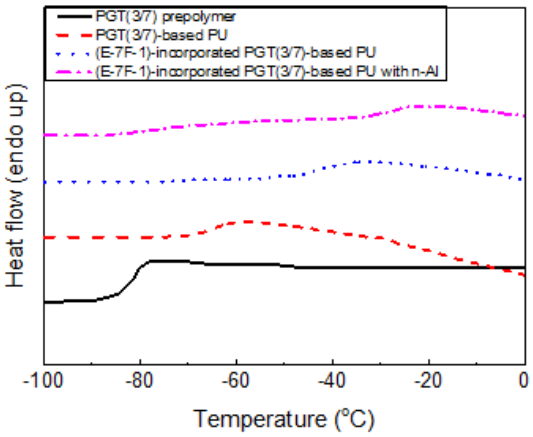

Fig. 4 DSC curves of PGT(3/7) prepolymer, PGT(3/7)-based PU, (E-7F-1)-incorporated PGT(3/7)-based PU and (E-7F-1)-incorporated PGT(3/7)-based PU with n-Al.

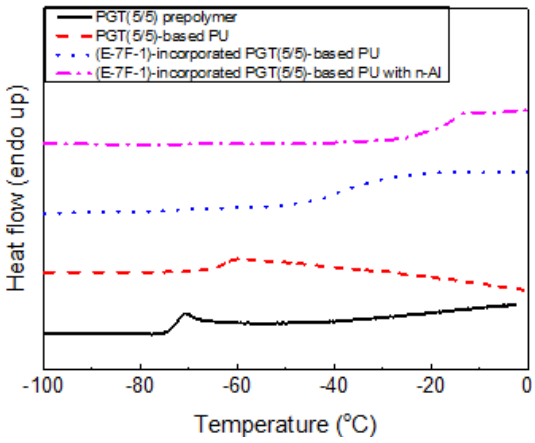

Fig. 5 DSC curves of PGT(5/5) prepolymer, PGT(5/5)-based PU, (E-7F-1)-incorporated PGT(5/5)-based PU and (E-7F-1)-incorporated PGT(5/5)-based PU with n-Al.

n-Al/(E-7F-1)-incorporated PGT(3/7)-based PU binders. However, (E-7F-1)-incorporated PGT(5/5))-based PU showed higher T_g, which was attributed to the structural composition of PGT prepolymer. PGT(5/5) prepolymer has more azide groups per unit mole than PGT(3/7) prepolymer, providing more reaction site for forming the triazole side groups and resulting in more rigid structure of FRP-incorporated PGT(5/5)-based PU. Importantly, it inferred from low T_g that these PU binders still maintained elastic characters at room temperature and could expect to show good elastic properties even at low temperature.

Table 2. DSC and TGA data of FRPs, PGT prepolymers, PGT-based PUs, FRP-incorporated PGT-based PUs and FRP-incorporated PGT-based PUs with n-Al.

Materials		T_g (°C)	$T_{d,max}$ (°C)
FRP	E-7F-1	-107.1	124.7
	E-7F-2	-105.1	118.9
	F-8F-1	-119.7	136.0
	F-8F-2	-114.2	145.9
PGT(3/7) prepolymer		-87.6	---
PGT(3/7)-based PU		-63.7	243.7
FRP-incorporated PGT(3/7)-based PU	E-7F-1	-39.8	403.3
	E-7F-2	-67.1	403.3
	F-8F-1	-60.3	370.8
	F-8F-2	-62.0	403.3
FRP-incorporated PGT(3/7)-based PU with n-Al(20 wt%)	E-7F-1	-27.5	403.3
	E-7F-2	-39.5	403.3
	F-8F-1	-49.4	370.8
	F-8F-2	-41.6	403.3
PGT(5/5) prepolymer		-72.5	---
PGT(5/5)-based PU		-62.7	238.8
FRP-incorporated PGT(5/5)-based PU	E-7F-1	-36.2	320.9
	E-7F-2	-51.8	336.0
	F-8F-1	-49.5	381.0
	F-8F-2	-51.2	393.4
FRP-incorporated PGT(5/5)-based PU with n-Al(20 wt%)	E-7F-1	-16.1	332.0
	E-7F-2	-25.1	385.4
	F-8F-1	-41.0	376.5
	F-8F-2	-26.8	366.7

Thermal stability was measured with TGA and summarized in Table 2. Fig. 6 shows a representative series of n-Al/(E-7F-1)-incorporated PGT(3/7)-based PU. Ester-linkage E-7F-1 FRP showed fast weight loss at 124.7°C, which was considered as the

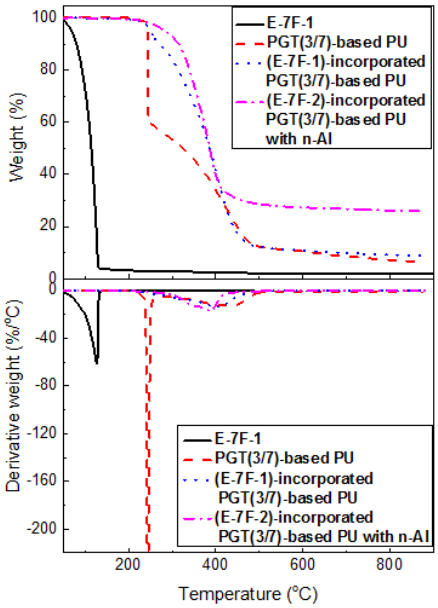

Fig. 6 TGA curves of E-7F-1, PGT(3/7)-based PU, (E-7F-1)-incorporated PGT(3/7)-based PU and n-Al/(E-7F-1)-incorporated PGT(3/7)-based PU.

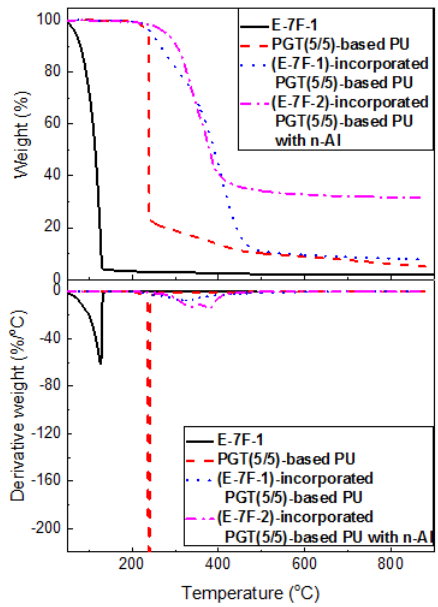

Fig. 7 TGA curves of E-7F-1, PGT(5/5)-based PU, (E-7F-1)-incorporated PGT(5/5)-based PU and n-Al/(E-7F-1)-incorporated PGT(5/5)-based PU.

evaporation because perfluorocarbons had lower boiling point than corresponding hydrocarbons [12]. PGT(3/7) prepolymer was decomposed at 243.7°C, attributed to azide groups in side chain of PGT, decomposing to release N_2 [13]. On the other hand, (E-7F-1)-incorporated PGT(3/7)-based PU, prepared by the PU reaction with in-situ click reaction, exhibited $T_{d,max}$ at 403.3°C, not showing any decomposition of respective PGT(3/7) and E-7F-1. It implied the formation of thermally stable triazole moiety by converting unstable azide group through the click reaction between the azide group of PGT and alkyne group of E-7F-1. In the case of n-Al/(E-7F-1)-incorporated PGT(3/7)-based PU, the remaining mass balance was due to n-Al and close to the prepared formulations.

Similar phenomena were observed in the series of PGT(5/5), as shown in Fig. 7. much dramatic weight loss of PGT(5/5)-based PU was observed at 238.8°C due to higher N_3 content than PGT(3/7) system and completely prevented after forming (E-7F-1)-incorporated PGT(5/5)-based PU. Further addition of n-Al in these systems had little effect on the thermal stability.

3.2 Energy performance

The energy performance of n-Al/FRP-incorporated PGT-based PU binders was investigated to evaluate the enthalpy of reaction (ΔH) by the thermite reaction using DSC. The maximum exothermic temperature (T_{max}) and ΔH were summarized in Table 3. Firstly, mixtures of FRP/n-Al were studied using DSC with Al crucible and high pressure crucible, respectively, as shown in Fig. 8. FRP/n-Al mixtures, measured using general Al crucible in Fig. 8(a), did not show considerable exothermic peaks, suggesting no thermite reaction. Due to the volatility of FRPs

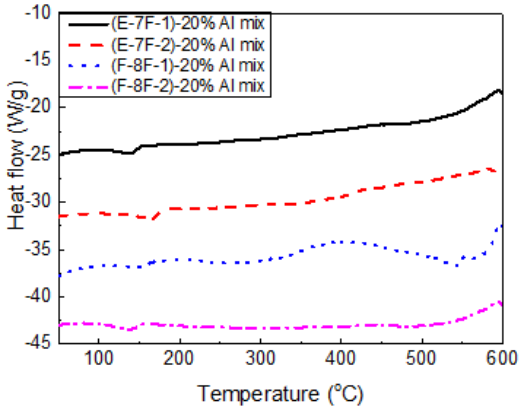

(a)

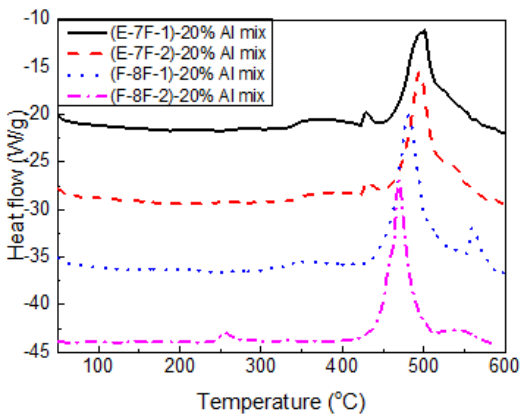

(b)

Fig. 8 DSC ((a) Al crucible and (b) high pressure crucible) curves of the mixture of nano-aluminum and FRPs, respectively.

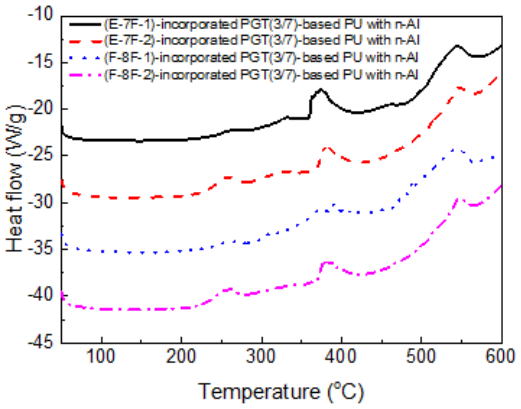

(a)

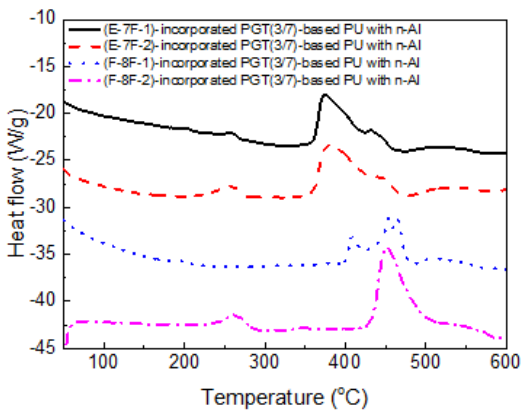

(b)

Fig. 9 DSC ((a) Al crucible and (b) high pressure crucible) curves of FRP-incorporated PGT(3/7)-based PU with n-Al.

Table 3. DSC data (high pressure crucible) of mixture of FRPs and n-Al.

Materials		T_{max} (°C)	ΔH (J/g)
FRP/n-Al(20 wt%)	E-7F-1	500.0	-2545.5
	E-7F-2	494.0	-2637.6
	F-8F-1	480.8	-3266.1
	F-8F-2	453.3	-2379.6

previously mentioned in TGA result, the general Al crucible could not be sealed in order to prevent any loss of gaseous FRPs. In order to better evaluate the thermite reaction, DSC was measured using a special high pressure crucible, which was strong enough to make the volatile FRPs remain inside the crucible and carry out complete thermite reaction with n-Al. Therefore, FRP/n-Al mixtures, measured using high pressure crucible, showed the thermite reaction of fluorine atoms and n-Al or Al_2O_3 to form AlF_3 in the temperature range of 410°C ~ 600°C [8,9,14], as illustrated in Fig. 8(b).

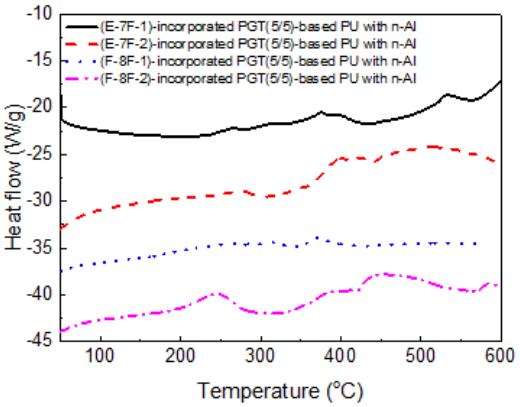

(a)

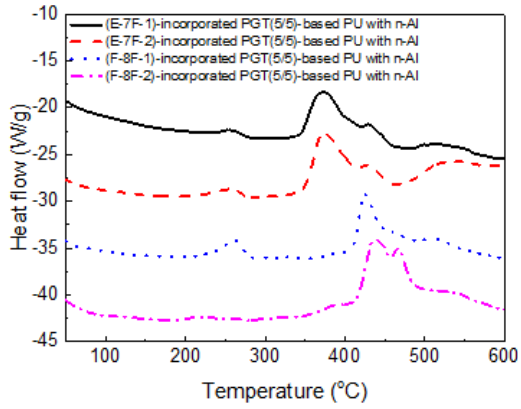

(b)

Fig. 10 DSC ((a) Al crucible and (b) high pressure crucible) curves of FRP-incorporated PGT(5/5)-based PU with n-Al.

Secondly, n-Al/FRP-incorporated PGT-based PUs were also investigated to evaluate the thermite reaction for both PGT(3/7) and PGT(5/5) systems, as presented in Fig. 9 and Fig. 10, and summarized in Table 4. Because DSC curves, measured using Al crucible, could hardly observe obvious exothermic peaks, DSC curves, measured using the high pressure crucible, were used to quantify the thermite reaction. In Fig. 9(b), T_{max}s of exothermic thermite reaction of n-Al/ester-linkage (E-7F-1 and E-7F-2) FRP-incorporated/PGT(3/7)-based PU were measured around 375°C ~ 378°C. On the other hand, n-Al/formal-linkage (F-8F-1 and F-8F-2) FRP-incorporated/PGT(3/7)-based PU showed T_{max}s around 428°C ~ 453°C. It appeared that ester-linkage FRP-incorporated systems showed the thermite reaction at lower temperature than formal-linkage FRP-incorporated ones, regardless of PGT(3/7) and PGT(5/5) used. However, ΔH of the thermite reaction seemed to be dependant on PGT, exhibiting PGT(5/5) were found to have higher ΔH value than PGT(3/7).

Table 4. DSC (High pressure crucible) data of FRP-incorporated PGT-based PUs with n-Al.

Materials		T_{max} (°C)	ΔH (J/g)
FRP-incorporated PGT(3/7)-based PU with n-Al(20 wt%)	E-7F-1	374.7	-1747.9
	E-7F-2	378.0	-1985.8
	F-8F-1	453.5	-1184.5
	F-8F-2	428.0	-3396.8
FRP-incorporated PGT(5/5)-based PU with n-Al(20 wt%)	E-7F-1	372.7	-4450.2
	E-7F-2	371.2	-3712.4
	F-8F-1	424.7	-4095.5
	F-8F-2	452.5	-1552.5

Heat of combustion ($\Delta H_{c,exp}$) was measured using Parr Bomb calorimeter. In order to compare ΔH_c measurement to theoretical predictions [10], the $\Delta H_{c,cal}$ for each sample was estimated using eq. 1.

$$\Delta H_{c,cal} = [wt\%active\ Al \times \Delta H_{Al}] + [wt\%PU \times \Delta H_{PU}] \quad (1)$$

The wt% active Al was found to be ~62% as determined by TGA (Fig. 11) by measuring the mass gain due to oxidation of aluminum via reaction between Al and O_2 ($4Al + 3O_2 \rightarrow 2Al_2O_3$). The PU in this equation means FRP-incorporated PGT-based PU.

Table 5 summarizes the ΔH_c, measured and calculated, of n-Al/(E-7F-1)-incorporated PGT(5/5)-based PU. The $\Delta H_{c,exp}$ of

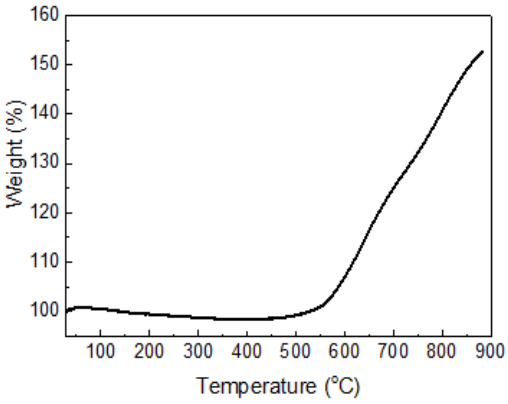

Fig. 11 TGA curve of nano aluminum particle.

Table 5. Summarized data of heat of combustion.

Materials	$\Delta H_{c,exp}$ (kJ/g)	$\Delta H_{c,cal}$ (kJ/g)
PGT(5/5) prepolymer	25.5	26.0
PGT(5/5) based PU	25.5	26.4
(E-7F-1)-incorporated PGT(5/5)-based PU with n-Al(20 wt%)	20.1	21.0

n-Al/(E-7F-1)-incorporated PGT(5/5)-based PU was 20.1 kJ/g, which was similar to the theoretical prediction ($\Delta H_{c,cal}$=21.0 kJ/g). It was reported [10] that the ΔH_c of epoxy samples with n-Al/PFPE was around 23.6 ~ 25.3 kJ/g, showing close results with our values.

4. Conclusions

Thermal characteristics of n-Al/FRP-incorporated PGT-based PU binders were measured to investigate the feasibility of fluorine groups as fundamentally inactive but potentially (latent) energetic group by the exothermic thermite reaction with aluminum in PBXs. n-Al/FRP-incorporated PGT-based PU binders were prepared by simultaneous polyurethane and catalyst-free azide-alkyne click reaction in the presence of nano-aluminum. Initial study carried out with n-Al/FRP mixtures using DSC with high pressure crucible pan demonstrated the thermite reaction at 450°C ~ 500°C. The thermite reaction of n-Al/FRP-incorporated PGT-based PU binders was measured at 370°C ~ 450°C, lower than n-Al/FRP mixtures. The enthalpy of thermite reaction measured implied n-Al/FRP-incorporated PGT-based PUs as the potential for an energetic PU binders. The n-Al/FRP-incorporated PGT-based PUs may further expand the use as a stand-alone energetics or as additives to other energetic systems with tailorable exothermic properties.

Acknowledgment

This study was supported by Next-Generation Converged Energy Materials Research Center (CEMRC)

References

1. Bohn, M.A., "Determination of the Kinetic Data of the Thermal Decomposition of Energetic Plasticizers and Binders by Adiabatic Self Heating," *Thermochimica Acta*, Vol. 337, No. 1-2, pp. 121-139, 1999.
2. Chen, Y., Kwon, Y. and Kim, J.S., "Synthesis and Characterization of Bis(2,2-dinitropropyl ethylene) Formal Plasticizer for Energetic Binders," *Journal of Industrial and Engineering Chemistry*, Vol. 18, No. 3, pp. 1069-1075, 2012.
3. Kumari, D., Yamajala, K.D.B., Singh, H., Sanghavi, R.R., Asthana, S.N., Raju, K. and Banerjee, S., "Application of Azido Esters as Energetic Plasticizers for LOVA

Propellant Formulations," *Propellants, Explosives, Pyrotechnics*, Vol. 38, No. 6, pp. 805-809, 2013.

4. Selim, K., Ozkar, S. and Yilmaz, L., "Thermal Characterization of Glycidyl Azide Polymer (GAP) and GAP-based Binders for Composite Propellants," *Journal of Applied Polymer Science*, Vol. 77, No. 3, pp. 538-546, 2000.
5. Koch, E.C., *Metal-Fluorocarbon Based Energetic Materials*, Wiley-VCH Verlag & Co. KGaA, Weinheim, Germany, 2012.
6. Yang, Y., Wang, S., Sun, Z. and Dlott, D.D., "Near-infrared Laser Ablation of Polytetrafluoroethylene (PTFE) Sensitized by Nanoenergetic Materials," *Applied Physics Letters*, Vol. 85, No. 9, pp. 1493-1495, 2004.
7. Fisher, S. and Grubelich, M., "A Survey of Combustible Metals, Thermites, and Intermetallics for Pyrotechnic Applications," *32nd Joint Propulsion Conference and Exhibit*, Lake Buena Vista, F.L., U.S.A., AIAA 1996-3018, Jul. 1996.
8. Pantoya, M.L. and Dean, S.W., "The Influence of Alumina Passivation on Nano-Al/Teflon Reactions," *Thermochimica Acta*, Vol. 493, No. 1-2, pp. 109-110, 2009.
9. Huang, C., Jian, G., DeLisio, J.B., Wang, H. and Zachariah, M.R., "Electrospray Deposition of Energetic Polymer Nanocomposites with High Mass Particle Loadings: A Prelude to 3D Printing of Rocket Motors," *Advanced Engineering Materials*, Vol. 17, No. 1, pp. 95-101, 2015.
10. Kettwich, S.C., Kappagantula, K., Kusel, B.S., Avjian, E.K., Danielson, S.T., Miller, H.A., Pantoya, M.L. and Lacono, S.T., "Thermal Investigations of Nanoaluminum/ Perfluoropolyether Core-Shell Impregnated Composites for Structural Energetics," *Thermochimica Acta*, Vol. 591, pp. 45-50, 2014.
11. Ma, M., Shen, Y., Kwon, Y., Chung, C. and Kim, J.S., "Reactive Energetic Plasticizers for Energetic Polyurethane Binders Prepared via Simultaneous Huisgen Azide-Alkyne Cycloaddition and Polyurethane Reaction," *Propellants, Explosives, Pyrotechnics*, Vol. 41, pp. 746-756, 2016.
12. Smart, B.E., "Fluorine Substituent Effects (on Bioactivity)," *Journal of Fluorine Chemistry*, Vol. 109, No. 1, pp. 3-11, 2001.
13. Ang, H.G. and Pisharath, S., *Energetic Polymers*, Wiley-VCH Verlag & Co. KGaA, Weinheim, Germany, 2012.
14. Miller, H.A., Kusel, B.S., Danielson, S.T., Neat, J.W., Avjian, E.K., Pierson, S.N., Budy, S.M., Ball, D.W., Iacono, S.T. and Kettwich, S.C., "Metastable Nanostructured Metallized Fluoropolymer Composites for Energetics," *Journal of Materials Chemistry A*, Vol. 1, No. 24, pp. 7050-7058, 2013.